Exploration of BioMat-X

Open Exploration

Open Access Original Article

Preparation and characterization of stearyl glycyrrhetinate/cyclodextrin complex using co-grinding

Momoko Ebisawa[1], Nao Kodama[1], Shun-ichi Mitomo[1], Junki Tomita[2], Mitsuaki Suzuki[3], Yutaka Inoue[1]*

[1]Laboratory of Nutri-Pharmacotherapeutics Management, Faculty of Pharmacy and Pharmaceutical Sciences, Josai University, Sakado 3500295, Japan

[2]Instrument Analysis Center, Josai University, Sakado 3500295, Japan

[3]Department of Chemistry, Faculty of Science, Josai University, Sakado 3500295, Japan

***Correspondence:** Yutaka Inoue, Laboratory of Nutri-Pharmacotherapeutics Management, Faculty of Pharmacy and Pharmaceutical Sciences, Josai University, 1-1 Keyakidai, Sakado, Saitama 3500295, Japan. yinoue@josai.ac.jp

Academic Editor: Jayachandran Venkatesan, Yenepoya University, India

Received: September 4, 2024 **Accepted:** February 10, 2025 **Published:** February 26, 2025

Cite this article: Ebisawa M, Kodama N, Mitomo Si, Tomita J, Suzuki M, Inoue Y. Preparation and characterization of stearyl glycyrrhetinate/cyclodextrin complex using co-grinding. Explor BioMat-X. 2025;2:101330. https://doi.org/10.37349/ebmx.2025.101330

Abstract

Aim: In this study, the physicochemical properties of stearyl glycyrrhetinate/β-cyclodextrin (SG/βCD) and SG/γCD complexes were characterized, and the complexes were prepared using the co-milling method. The molecular interactions within the SG/CD complexes were also investigated using nuclear magnetic resonance (NMR) measurements to determine the mode of interaction.

Methods: Here, we evaluated the physicochemical properties of SG complexes with CDs prepared by ground mixtures (GM SG/βCD or γCD = 1/1, 1/2).

Results: Powder X-ray diffraction (PXRD) showed that the characteristic SG and CD peaks disappeared after co-grinding with GM (SG/CD = molar ratio of 1/2), indicating a halo pattern. Differential scanning calorimetry (DSC) measurements showed that after co-grinding, the endothermic peak due to SG melting, as well as the dehydration peak and the endothermic peak due to SG melting, disappeared. Near-infrared (NIR) spectroscopy results showed that the peaks of SG-derived –CH moieties and CD-derived –OH and –CH moieties broadened in GM, suggesting their involvement in complex formation through SG/CDs intermolecular interactions. In GM (SG/CDs), NMR measurements showed broadened H-A and H-F peaks of the steroid skeleton derived from SG. In GM (SG/βCD = 1/2), the doublet peak, especially OH-3 at the wide edge of CD, shifted to a singlet peak. In GM (SG/γCD = 1/2), the H-3 peak, which is the wide edge of γCD, and the H-6 peak, which is the narrow edge, shifted to broad peaks, suggesting that γCD is deeply encapsulated in the steroidal structure.

Conclusions: These findings suggest that complex formation occurred in SG/CDs and that inclusion behavior is different between GM (SG/βCD = 1/2) and GM (SG/γCD = 1/2).

Keywords

Stearyl glycyrrhetinate, cyclodextrin, co-grinding, inclusion, nuclear magnetic resonance

Introduction

The epidemic of new coronavirus infection has made wearing masks a habit, leading to an increasing number of people experiencing skin problems such as mask-induced steaming, acne, and pimples [1]. Skincare products are often used as a countermeasure against skin problems, and a few of these products contain ingredients that prevent skin irritation. One example is stearyl glycyrrhetinate (SG), a derivative of 18-β-glycyrrhetinic acid (GA), a major metabolite of glycyrrhizic acid (GL) found in licorice root [2, 3]. SG is a dehydration-condensed ester of the hydroxyl group of stearyl alcohol on the carboxyl group of GL. SG is more lipophilic than dipotassium glycyrrhizinate [4], another derivative of GL, and is used in cosmetics such as creams and emulsions [5]. It has anti-inflammatory, skin-soothing, and antioxidant properties [6]. However, the physical properties of SG render them poorly soluble in water, necessitating a formulation that improves its solubility.

Cyclodextrin (CD) is a cyclic oligosaccharide composed of α-1,4-linked D-glucopyranose with a conical hydrophobic inner cavity and a hydrophilic outer surface. The natural CD varieties include those with at least six glucose units, with the most common CDs those that present six (αCD), seven (βCD), and eight units (γCD) [7]. Their compounds, cyclodextrins (α-, β-, and γ-CDs), are "generally recognized as safe" by the U.S. Food and Drug Administration (FDA), according to Braga et al. [8]. For these advantages in drug delivery, various CDs, including α-, β-, and γ-CDs, have already been registered as pharmaceutical excipients. The cavities of CDs are slightly hydrophobic and can incorporate lipophilic drugs and moieties. CDs have a three-dimensional shape like a hollow torus and exhibit different polarities on their inner and outer surfaces [9]. These primary and secondary hydroxyl moieties are located on the narrow and wide sides, respectively. In this sense, the primary hydroxyl moieties can rotate and reduce the diameter of CDs, whereas the secondary hydroxyl moieties form strong hydrogen bonds and give the CDs rigidity [10]. Due to their special structures, CDs can encapsulate guest molecules and form inclusion complexes. The inclusion complexation of hydrophobic compounds primarily occurs through hydrophobic interactions between the CD cavity wall and guest molecules. Other forces, such as dipole-dipole interactions and van der Waals interactions, may also contribute to guest binding [11]. Complex formation improves the water solubility of drugs, increases chemical stability [12], reduces or prevents irritation, and masks unpleasant tastes and odors [13]. Our laboratory has reported that the formation of a complex between the pentacyclic triterpenoid ursolic acid and γCD enhanced solubility [14]. The inclusion complexes were prepared using a mechanochemical mixture.

Current studies suggest that SG/CD inclusion complexes can be prepared by co-grinding SG with CDs and that the physicochemical properties of SG may be modified, leading to the functional improvement of SG. This contributes to the anti-inflammatory effect of SG on mask rash and rough skin with improved formulation handling. In this study, it is proposed that co-grinding SG with CD to modify its physicochemical properties and prepare SG/CD complexes could expand the potential for improving SG functionality. Specifically, this approach may enhance the handling properties of SG formulations and further contribute to the anti-inflammatory effects of SG against mask-induced skin irritation and other skin problems. Therefore, in this study, SG/βCD and SG/γCD were co-grinding to form complexes with poorly soluble drugs. Then, SG/CDs complexes were prepared and the intermolecular interactions in the solid state were investigated by nuclear magnetic resonance (NMR) measurements to evaluate the physical properties and the mode of complex formation.

Materials and methods

Materials

The SG was purchased from Tokyo Chemical Industry Co., Ltd. (Lot. TUWLL-ID, Tokyo, Japan). βCD and γCD were donated by CycloChem Bio Co., Ltd. (Tokyo, Japan) and stored at 40°C and 82% relative humidity for 7 days (Figure 1). NMR solvents were purchased from Fujifilm Wako Pure Chemical Corporation (Tokyo, Japan). Other reagents were purchased from Fujifilm Wako Pure Chemical Corporation.

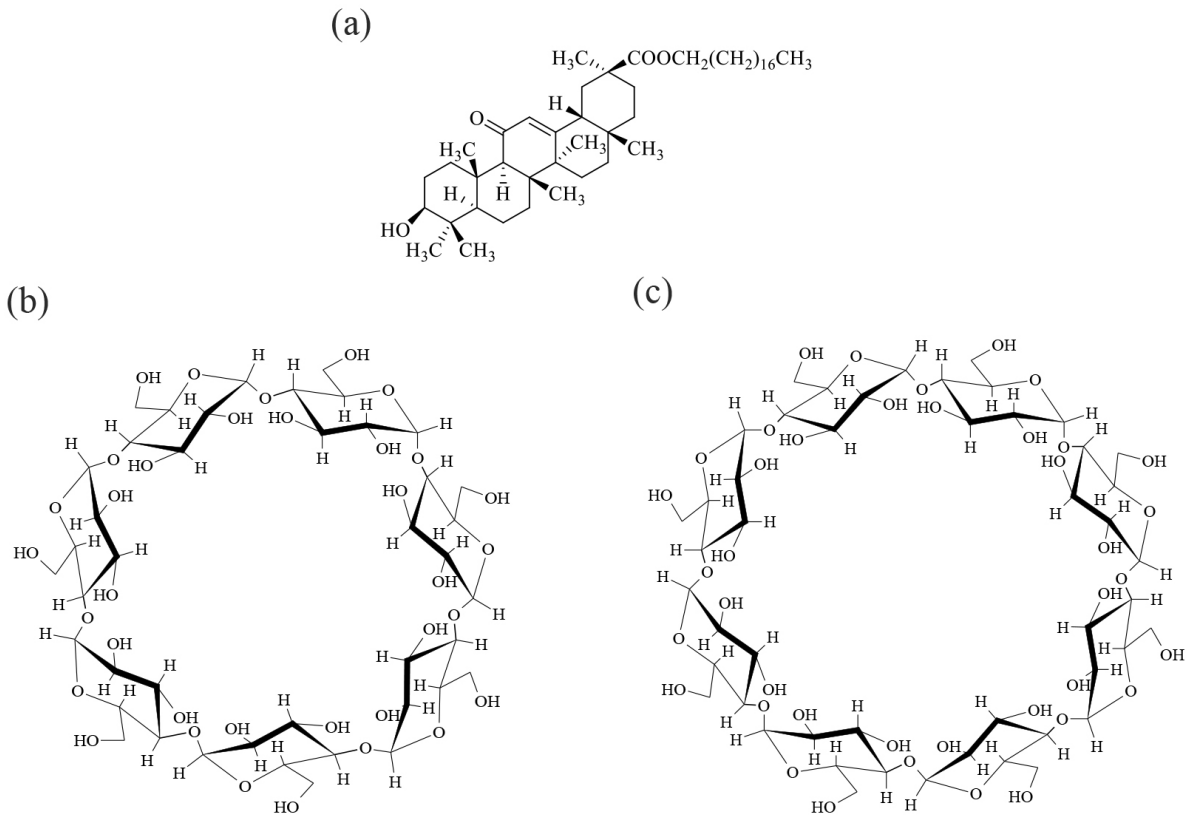

Figure 1. Chemical structure of (a) SG, (b) βCD, and (c) γCD. SG: stearyl glycyrrhetinate; CD: cyclodextrin

Sample preparation

Physical mixtures (PM) were prepared by weighing SG and βCD or γCD in a molar ratio of 1/1 or 1/2, respectively, and mixing them in a vortex mixer for 1 min. Ground mixtures (GM) were prepared by weighing out a total of 500 mg of PM (SG/βCD, SG/γCD) and grinding it in a vibrating rod mill (TI-500ET, CMT Co., Ltd., Tokyo, Japan) for 30 min.

Powder X-ray diffraction (PXRD) measurement

Diffraction intensity was measured with a NaI scintillation counter using a Miniflex II powder X-ray diffraction measuring device (Rigaku Corporation, Tokyo, Japan). The measurement conditions used were Cu radiation (30 kV, 15 mA), a scan condition of 4°/min for the X-ray diffraction measurement, and a measurement range of 2θ = 5–40°. The measurements were performed by filling a powdered sample into a glass plate; therefore, the sample plane was flat.

Differential scanning calorimetry (DSC) measurements

Measurements were performed using a high-sensitivity differential scanning calorimeter (Thermo Plus Evo; Rigaku Corporation, Tokyo, Japan). A sample weighing 1.5–2 mg was precisely measured and placed in a sealed aluminum pan for analysis. The measurement conditions were nitrogen gas flow rate of 60 mL/min, temperature increase rate of 10.0 °C/min, and measurement range of 30–350°C.

Near-infrared (NIR) absorption spectrum measurement

Measurements were performed using a Fourier-transform near-infrared spectrometer (JASCO V-770; JASCO Corporation, Tokyo, Japan). Approximately 3 mg of each sample was placed in a powder cell for measurement, and measurements were performed at 5 nm intervals along the optical path. Measurement conditions were a measurement range of 4,000–10,000 cm^{-1}, measurement time of 8 s, and measurement temperature of 25°C. The obtained spectra were subjected to second-order differentiation and analysis.

Scanning electron microscopy (SEM)

SEM measurements were performed using a JSM-IT800 (SHL) instrument (JEOL, Tokyo, Japan) at an accelerating voltage of 1 kV. The vacuum gold steaming time of the samples was 60 s.

^{1}H-NMR spectrum measurement

NMR spectroscopy was performed using an AVENCE NEO 600 cryosystem (Bruker, Yokohama, Japan) operating at 600.13 MHz in DMSO-d_6. The other conditions were as follows: 90° pulse, 7.775 μs; waiting time, 1 s; integration frequency, 64; and temperature, 25°C. Note: SG is a pentacyclic triterpenoid with low solubility in aqueous media. Therefore, SG was first dissolved in DMSO-d_6, and then diluted in aqueous media to be used in the NMR assay [15].

Results

PXRD measurement

The crystalline state of the SG/CDs (molar ratio of 1/1, 1/2) prepared by co-grinding was confirmed via PXRD measurements. Characteristic diffraction peaks were observed for intact SG at 2θ = 6.7°, 10.3°, 13.9°, and 17.5° (Figure 2a); βCD 2θ = 8.8° and 12.5° (Figure 2b); and γCD 2θ = 12.2°, 13.8°, and 16.3° (Figure 2g). Characteristic diffraction peaks derived from SG and CDs were observed for PM [SG/CDs (molar ratio of 1/1, 1/2)] (Figure 2c, d, h, i). In GM (SG/βCD = 1/1) and GM (SG/γCD = 1/1), the diffraction peaks derived from SG did not disappear (Figure 2e, j). In GM (SG/βCD = 1/2) and GM (SG/γCD = 1/2), the characteristic diffraction peak derived from SG disappeared. Furthermore, the diffraction peaks derived from βCD and γCD disappeared, and a halo pattern was exhibited (Figure 2f, k).

DSC analysis

The PXRD analysis results confirmed a halo pattern for GM (SG/CD = 1/2) in the solid state. Therefore, DSC analysis was carried out to determine the thermal behavior of GM (SG/βCD, SG/γCD). An endothermic peak due to the melting point of SG was observed at approximately 80°C for intact SG (Figure 3a). In βCD, an endothermic peak due to dehydration was observed at approximately 109°C, and a peak due to decomposition of βCD was observed at approximately 310°C (Figure 3b). In γCD, an endothermic peak due to dehydration was observed at approximately 72° to 101°C (Figure 3g). In PM (SG/βCD = 1/1, 1/2, SG/γCD = 1/1, 1/2) and GM (SG/βCD = 1/1, SG/γCD = 1/1), an endothermic peak due to the melting point of SG was observed at approximately 72°C (Figure 3c, d, e, h, i, j). Above 300°C, a peak of decomposition due to βCD or γCD was observed. In contrast, the disappearance of the endothermic peak due to SG was observed in GM (SG/βCD = 1/2, SG/γCD = 1/2) (Figure 3f, k).

NIR analysis

The results of PXRD and DSC indicated that GM (SG/βCD = 1/2) and GM (SG/γCD = 1/2) in the solid state formed inclusion complexes at a molar ratio of 1/2, respectively. To confirm the intermolecular interactions between SG/βCD and SG/γCD in the solid state, NIR absorption spectroscopy was performed (Figures 4, 5). This analysis is particularly useful for detecting CH, NH, and OH groups [16]. The CH-derived peaks of SG were identified at 4,367 cm^{-1}. The OH group peaks of βCD were observed at 4,808 cm^{-1} and 6,920 cm^{-1}, while the water content peak of βCD was observed at 5,208 cm^{-1} (Figure 4). In PM (SG/βCD = 1/2), the peak derived from –CH of SG was observed at 4,367 cm^{-1}, and no shift was observed in βCD. In GM (SG/βCD = 1/2), the peak of 4,367 cm^{-1} derived from the CH group of SG was observed to shift to 4,386 cm^{-1} at a higher

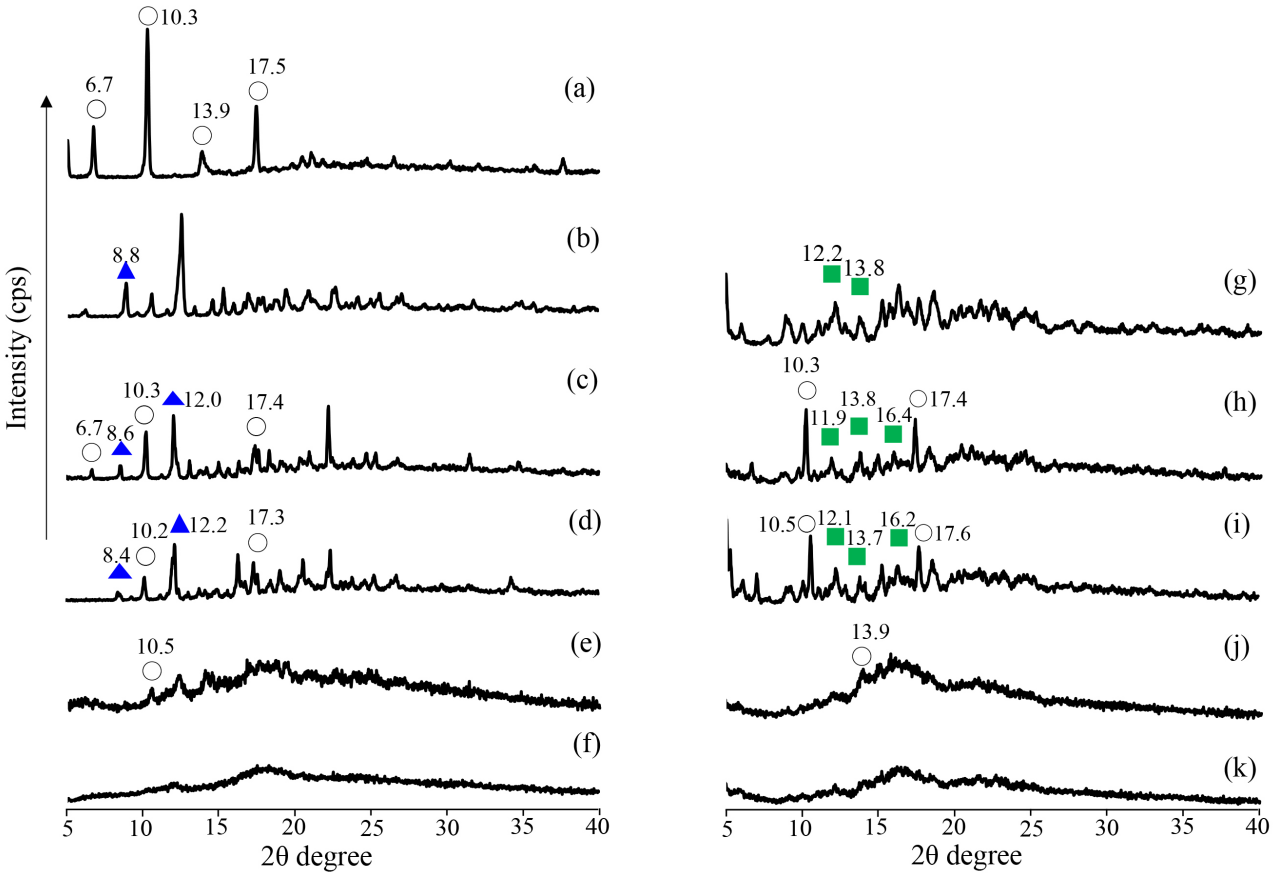

Figure 2. PXRD patterns of SG intact, SG/βCD, and SG/γCD systems. (**a**) SG intact, (**b**) βCD intact, (**c**) PM (SG/βCD = 1/1), (**d**) PM (SG/βCD = 1/2), (**e**) GM (SG/βCD = 1/1), (**f**) GM (SG/βCD = 1/2), (**g**) γCD intact, (**h**) PM (SG/γCD = 1/1), (**i**) PM (SG/γCD = 1/2), (**j**) GM (SG/γCD = 1/1), (**k**) GM (SG/γCD = 1/2). SG: stearyl glycyrrhetinate; CD: cyclodextrin; GM: ground mixtures; PM: physical mixtures. Open circle: SG original; blue solid triangle: βCD original; green solid square: γCD original

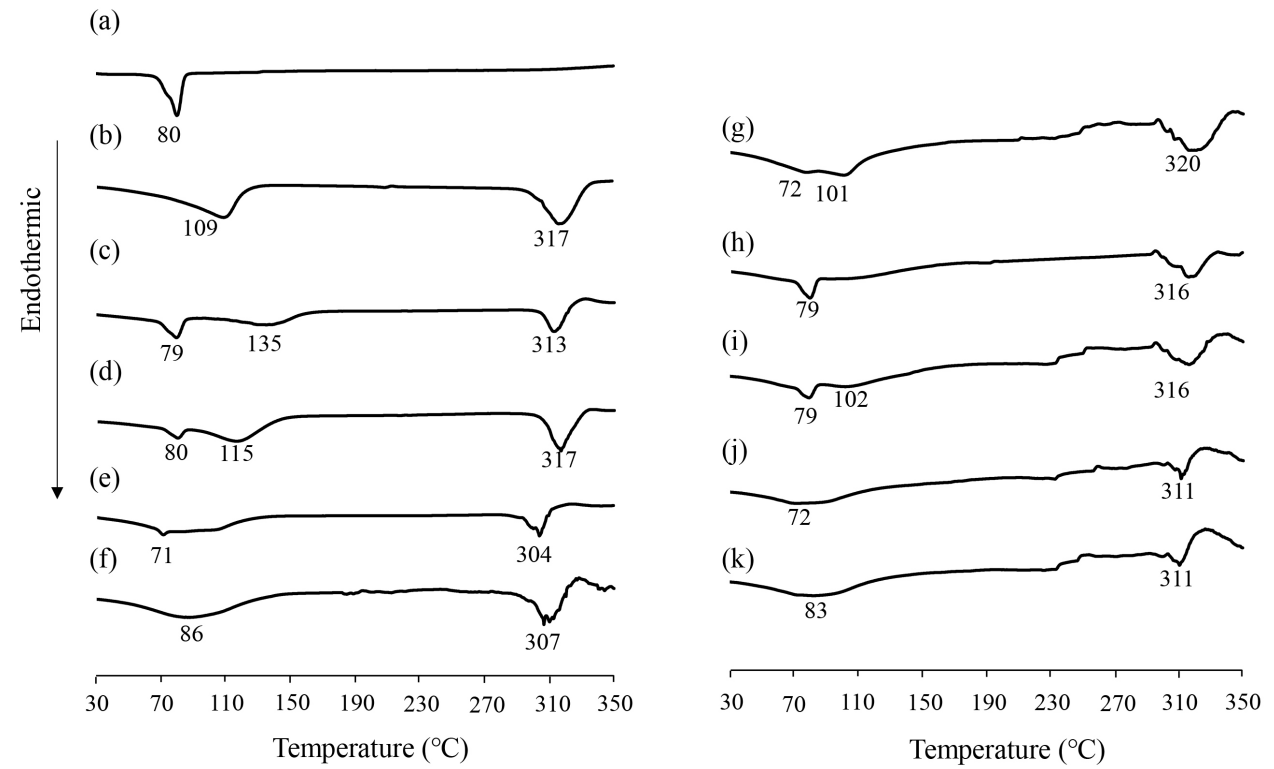

Figure 3. DSC curves of SG intact, SG/βCD, and SG/γCD systems. (**a**) SG intact, (**b**) βCD intact, (**c**) PM (SG/βCD = 1/1), (**d**) PM (SG/βCD = 1/2), (**e**) GM (SG/βCD = 1/1), (**f**) GM (SG/βCD = 1/2), (**g**) γCD intact, (**h**) PM (SG/γCD = 1/1), (**i**) PM (SG/γCD = 1/2), (**j**) GM (SG/γCD = 1/1), (**k**) GM (SG/γCD = 1/2). Heating rate: 10 °C/min. SG: stearyl glycyrrhetinate; CD: cyclodextrin; GM: ground mixtures; PM: physical mixtures

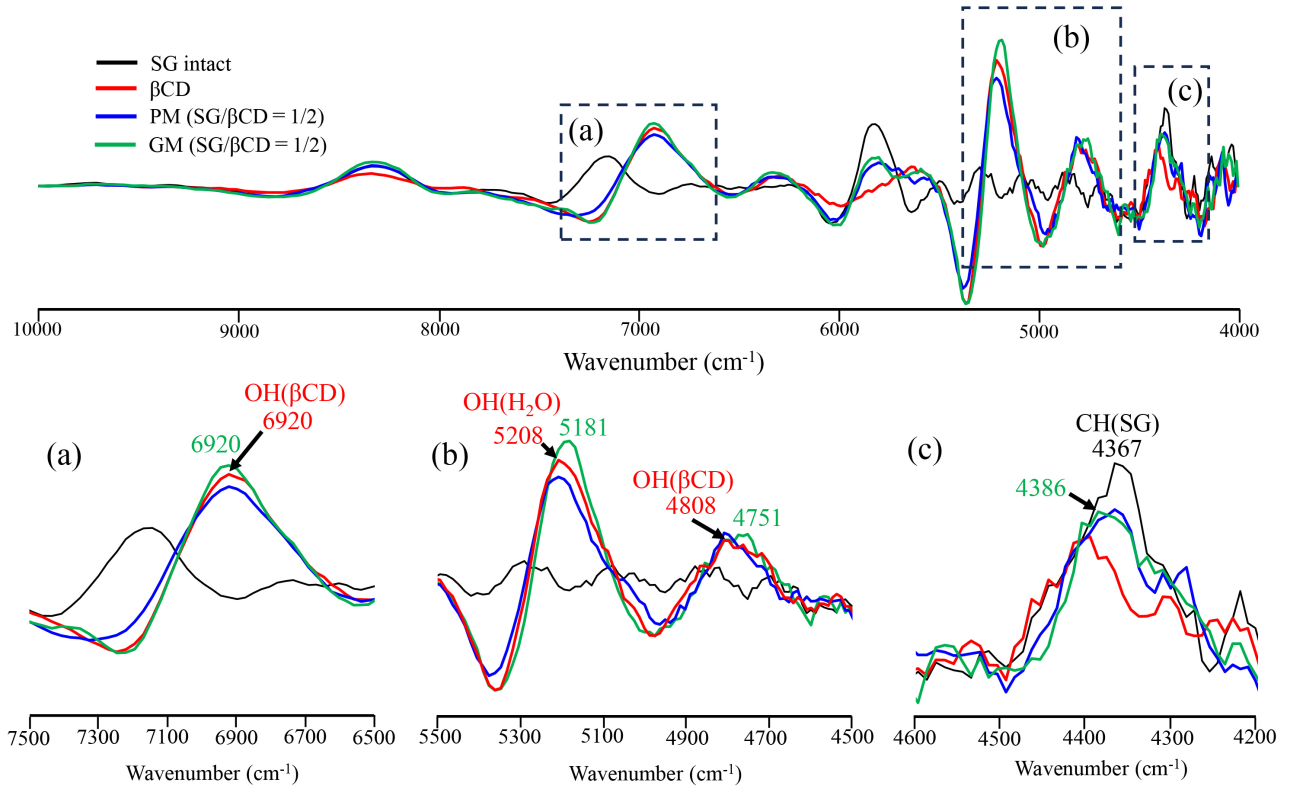

Figure 4. Second differentiation NIR absorption spectra of SG/βCD systems. (**a**) 7,500–6,500 cm^{-1}, (**b**) 5,500–4,500 cm^{-1}, (**c**) 4,600–4,200 cm^{-1}. SG: stearyl glycyrrhetinate; CD: cyclodextrin; GM: ground mixtures; PM: physical mixtures

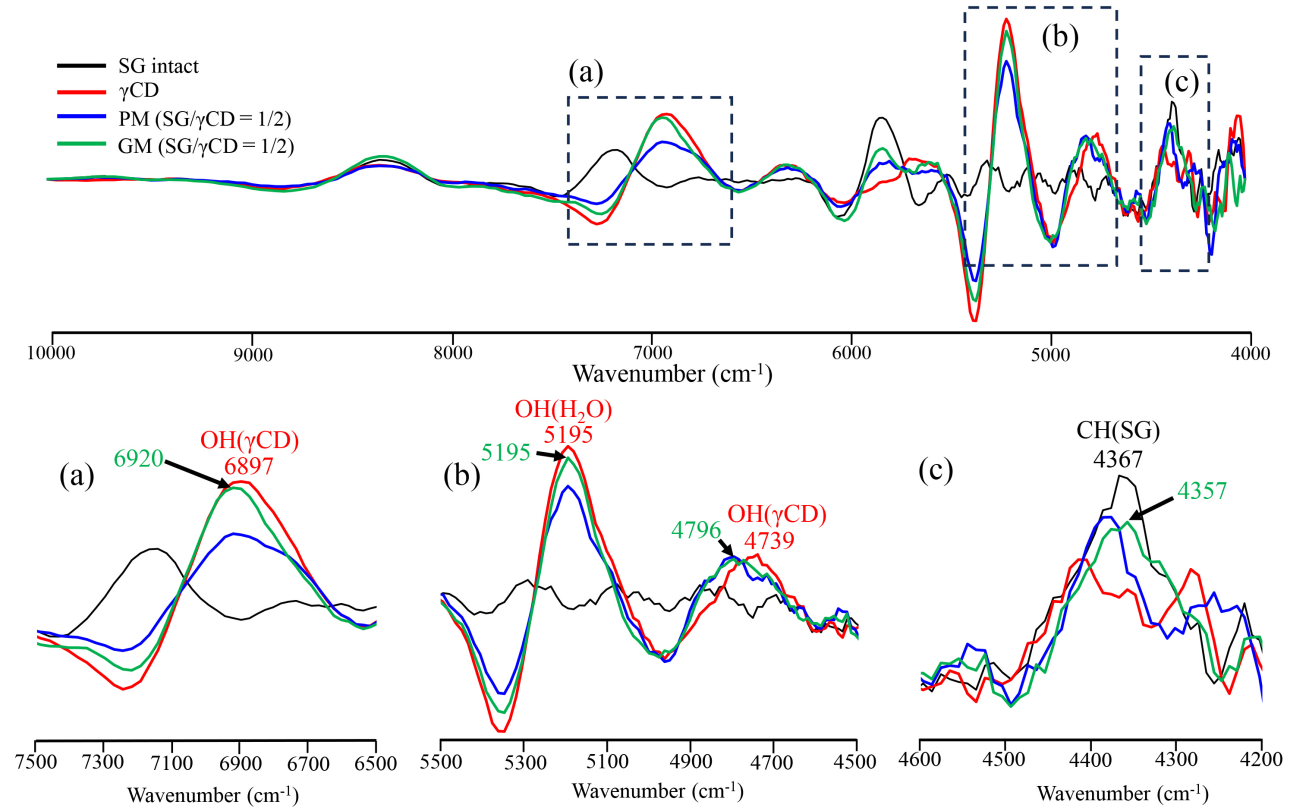

Figure 5. Second differentiation NIR absorption spectra of SG/γCD systems. (**a**) 7,500–6,500 cm^{-1}, (**b**) 5,500–4,500 cm^{-1}, (**c**) 4,600–4,200 cm^{-1}. SG: stearyl glycyrrhetinate; CD: cyclodextrin; GM: ground mixtures; PM: physical mixtures

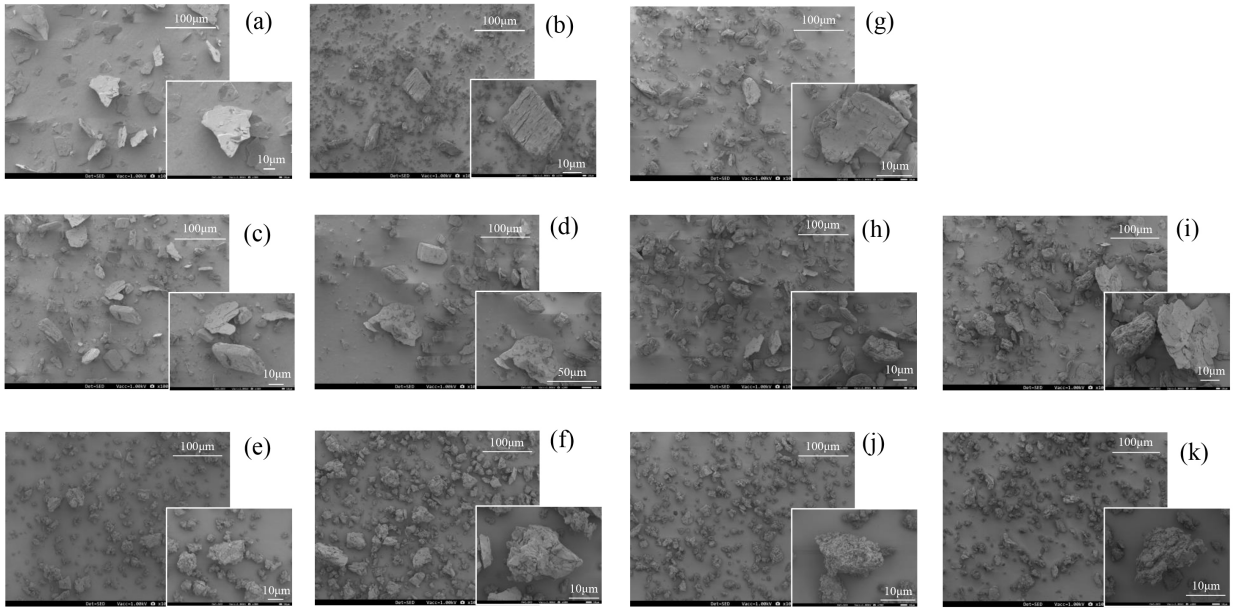

Figure 6. Scanning electron microscope images of SG intact, SG/βCD, and SG/γCD systems. (**a**) SG intact, (**b**) βCD intact, (**c**) PM (SG/βCD = 1/1), (**d**) PM (SG/βCD = 1/2), (**e**) GM (SG/βCD = 1/1), (**f**) GM (SG/βCD = 1/2), (**g**) γCD intact, (**h**) PM (SG/γCD = 1/1), (**i**) PM (SG/γCD = 1/2), (**j**) GM (SG/γCD = 1/1), (**k**) GM (SG/γCD = 1/2). SG: stearyl glycyrrhetinate; CD: cyclodextrin; GM: ground mixtures; PM: physical mixtures

wavenumber. In addition, the peak derived from the –OH group of βCD shifted to a lower wavenumber of 4,751 cm^{-1}, and the peak derived from the water content of βCD shifted to a lower wavenumber of 5,181 cm^{-1}. The OH group peaks of γCD were observed at 4,739 cm^{-1} and 6,897 cm^{-1}, and the water-containing peak of γCD was observed at 5,195 cm^{-1} (Figure 5). In PM (SG/γCD = 1/2), the peak derived from –CH of SG was observed at 4,357 cm^{-1}, and no shift was observed in γCD. In GM (SG/γCD = 1/2), the peak derived from the CH group at 4,357 cm^{-1} was observed to shift to a lower wavenumber at 4,367 cm^{-1}. In addition, the OH group peak of γCD related to 4,739 cm^{-1} was confirmed to shift to a higher wavenumber at 4,796 cm^{-1}. Although no peak shift was observed in the water-containing peak of γCD observed at 5,195 cm^{-1}, the peak was broadened. The peak of the OH group of γCD at 6,897 cm^{-1} was observed to shift to a higher wavenumber at 6,920 cm^{-1}.

Assessment of morphology via SEM

SEM measurements were performed to examine the morphology of SG/CDs (Figure 6). The surface of SG was observed to be flat, with small debris adhering to larger, thinner debris (Figure 6a). In βCD and γCD, smooth and angular surfaces were observed with a size of about 50–80 μm. (Figure 6b, g). In PM, the crystals of SG, βCD, and γCD were 50 μm in diameter, rough, and angular (Figure 6c, d, h, i). Generally, inclusions formed by CDs have been described as cubic [17]. In GM (SG/βCD = 1/1) and GM (SG/γCD = 1/1), angular cubic particles that looked like aggregates of small fragments 30 μm in diameter were observed, as well as cubic crystals in GM (SG/βCD = 1/2) and GM (SG/γCD = 1/2) (Figure 6e, f, j, k).

^{1}H-NMR spectrum measurement

In the solid state, PXRD, DSC, and NIR measurements suggested that SG formed an inclusion complex with the CDs. ^{1}H NMR spectroscopy was performed to predict the relative interactions between SG and CDs. Proton NMR measurements were performed to examine the intermolecular interactions in the solution. The results of GM (SG/βCD = 1/2) (DMSO-d_6) are shown in Figure 7. In intact SG, H-A was observed at approximately 2.98–3.03 ppm, and the H-F moiety derived from hydroxyl moieties was observed at approximately 4.25 ppm. In intact CD, H-3,5,6 derived from the CD cavity was observed at approximately 3.50 to 3.62 ppm. Furthermore, OH-2,3,6 (OH-2: 5.71 ppm, OH-3: 5.66 ppm, OH-6: 4.44 ppm) derived from outside the βCD cavity were observed [18]. In PM (SG/βCD = 1/1) and PM (SG/βCD = 1/2), SG intact and βCD-derived proton peaks were observed, and no change in peaks was observed. Similarly, no change in the peaks was observed in GM (SG/βCD = 1/1) and GM (SG/βCD = 1/2).

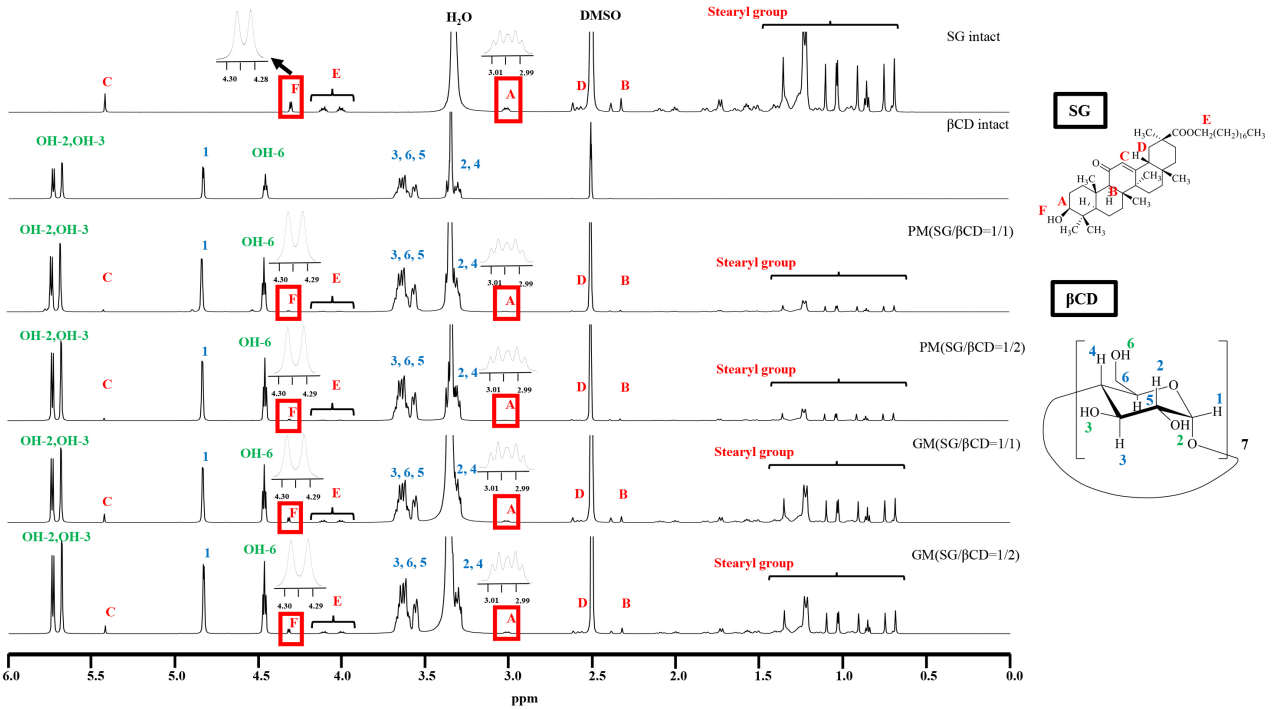

Figure 7. ^{1}H-NMR spectra of SG/βCD systems (DMSO-d_6). SG: stearyl glycyrrhetinate; CD: cyclodextrin; GM: ground mixtures; PM: physical mixtures

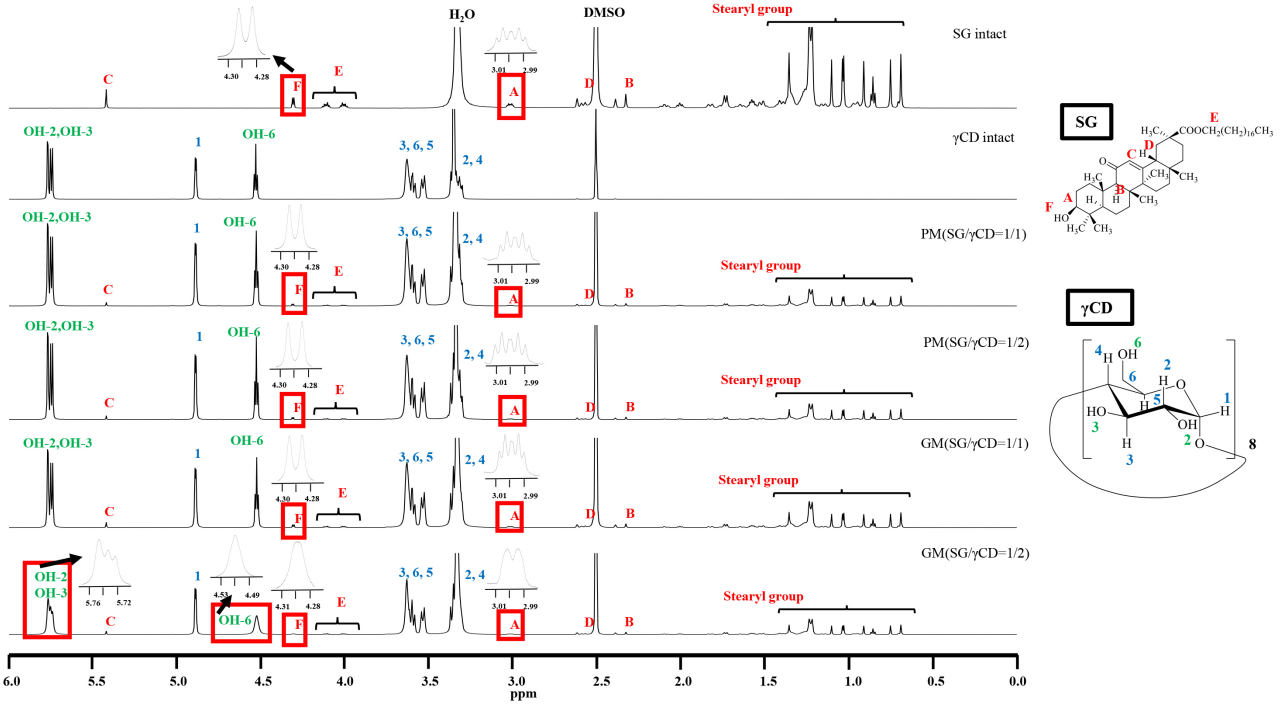

Figure 8. ^{1}H-NMR spectra of SG/γCD systems (DMSO-d_6). SG: stearyl glycyrrhetinate; CD: cyclodextrin; GM: ground mixtures; PM: physical mixtures

The results of GM (SG/γCD = 1/2) (DMSO-d_6) are shown in Figure 8. In γCD, H-3, H-5, and H-6 protons within the CD cavity were observed in the range of 3.50 to 3.62 ppm, while the OH-2, OH-3, and OH-6 protons outside the CD cavity appeared at approximately 5.75, 5.73, and 4.51 ppm, respectively. For PM (SG/γCD = 1/1) and PM (SG/γCD = 1/2), intact SG and γCD-derived proton peaks were detected, with no significant shifts observed. However, in GM (SG/γCD = 1/1), the H-3 and H-6 peaks of γCD within its cavity (3.50–3.69 ppm) shifted slightly downfield (H-3: from 3.61 to 3.62 ppm, H-6: from 3.58 to 3.59 ppm). In GM (SG/γCD = 1/2), the H-3 and H-6 peaks within the γCD cavity (3.56–3.64 ppm) also showed a downfield shift (H-3: from 3.61 to 3.62 ppm, H-6: from 3.58 to 3.59 ppm). Additionally, peak shifts were observed for

the H-A (2.98–3.03 ppm) and H-F (4.29 ppm) protons in SG, as well as for the OH-2 (5.75 ppm), OH-3 (5.73 ppm), and OH-6 (4.51 ppm) protons of γCD. Interestingly, the OH-2 and OH-3 peaks of γCD changed from sharp signals to broad peaks, while the OH-6 peak transitioned from a sharp triplet to a broad peak. Notably, the H-A and H-F peaks of SG also exhibited significant broadening (H-A: multiple peaks to broad doublet peaks, H-F: doublet peak to broad peak) in GM (SG/γCD = 1/2).

Discussion

The results of PXRD measurements showed that the characteristic diffraction peaks of SG, βCD, and γCD disappeared in GM (SG/βCD = 1/2) and GM (SG/γCD = 1/2), indicating a halo pattern [19, 20]. Furthermore, co-grinding can cause disorders due to the breakdown of the crystalline structure, and these amorphous solids exhibit halo patterns. When the PXRD pattern of a poorly soluble drug exhibits a halo pattern, it indicates that the material is in an amorphous state. In the amorphous state, molecules are arranged in a disordered manner compared to the ordered structure of crystalline solids. This state has higher energy, which enhances interactions with solvents and is expected to improve solubility compared to crystalline materials. In this study, mechanochemical treatment is specifically proposed to modify the surface energy of drug particles, thereby increasing their affinity with solvents. Therefore, mechanical energy in the form of distortion or percussion may induce mechanochemical interactions between SG and βCD in the solid state [21].

The DSC results of GM (SG/βCD = 1/2) and GM (SG/γCD = 1/2) showed the disappearance of the endothermic peak of SG and the decrease of the dehydration-derived peak of CD, suggesting the formation of an inclusion complex [16, 22]. This was presumably due to the loss of water from the CD, which was not involved in the inclusion complex. Thermal analysis showed changes in the thermal behavior, and the above findings suggest intermolecular interactions between GM (SG/CDs) and changes in the SG properties. The PXRD and DSC results suggested that SG/CD complexes may be formed at an SG/CD molar ratio of 1/2. Therefore, to confirm the intermolecular interactions of SG/βCD and SG/γCD in the solid state, NIR absorption spectroscopy, which is useful for analyzing the −CH and OH groups, was performed [23]. The results of the NIR measurements suggest that both GM (SG/βCD = 1/2) and GM (SG/γCD = 1/2) have significant peak shifts of the CH groups of SG and the OH moieties of the cavities of βCD and γCD, suggesting that molecular interaction occurs by inclusion in the CD cavities. In SEM observation, generally, when CDs form inclusion complexes, cubic crystals are reported to appear. In the GM of SG/CDs (1/1), the particle size was reduced to around 30 μm due to milling, and the particles exhibited a cubic shape with fine surface attachments, suggesting the formation of an inclusion complex.

The ^{1}H-NMR spectra measurement results showed no peak shift in GM (SG/βCD = 1/1 and 1/2). However, in GM (SG/γCD = 1/2), it was observed that the OH-2,3,6 peaks of γCD were broadened. In particular, in GM (SG/γCD = 1/2), the broadening of the H-A and H-F peaks of SG suggests an interaction involving the steroid skeleton containing H-A and H-F. Moreover, the wider ring structure of γCD compared to βCD may facilitate more effective encapsulation of the steroid skeleton of SG. We have previously reported that the inclusion complex of ursolic acid (which also has a steroid skeleton) with γCD adopts an inclusion mode where UA is encapsulated from the narrow edge of the CD [16]. Based on these findings, we speculate that in solution, GM (SG/γCD = 1/2) forms a complex with a CD:2 interaction involving the stearyl group of SG, along with potential interactions between the steroid backbone and γCD. Furthermore, the complex formation behavior appears to differ between GM (SG/βCD = 1/1 and 1/2) and GM (SG/γCD = 1/1 and 1/2). As a next step, we will try single crystal structure analysis as a promising method for structural analysis of SG/CD complexes, which will greatly facilitate the discussion and interpretation of NMR results that strongly support the present results.

Limitations of the present study include the fact that it is generally recommended to examine the solubility phase diagram and the inclusion of molar ratio by Job's plot to elucidate the complex formation between CD and the drug. However, as a limitation of our study, we could not quantify SG because its solubility in water was too low [SG < 0.5 μg/mL (D.W.)]. In addition, SG was not soluble in D_2O in NMR

measurement, and the proton peak by NMR measurement could not be detected. Therefore, DMSO-d_6 was used. Therefore, in this study, the complex was not prepared by the solution method, but by the GM method using mechanochemical processes, and physical properties in the solid state were evaluated as a basic step, followed by the elucidation of intermolecular interactions by NMR techniques. It is necessary to establish a quantitative method other than HPLC to confirm the solubility of SG. Alternatively, as a next research topic, preparing complexes using CD derivatives (e.g., HP-βCD and SBE-βCD) may help improve solubility. In the future, the SG/CD complexes obtained in this study could be further investigated for their anti-inflammatory effects and solubility. This would contribute to skin application research, addressing issues such as rough skin and other skin problems.

Abbreviations

CD: cyclodextrin

DSC: differential scanning calorimetry

GA: 18-β-glycyrrhetinic acid

GL: glycyrrhizic acid

GM: ground mixtures

NIR: near-infrared

NMR: nuclear magnetic resonance

PM: physical mixtures

PXRD: powder X-ray diffraction

SEM: scanning electron microscopy

SG: stearyl glycyrrhetinate

Declarations

Acknowledgments

The authors are grateful to Cyclo Chem Bio Co., Ltd. for providing the cyclodextrin samples. The authors wish to thank the Instrument Analysis Center of Josai University for helpful advice regarding NMR spectroscopy. We thank the Laboratory of Nutri-Pharmacotherapeutics Management, Josai University, for research support while taking measures against COVID-19 (SARS-CoV2) infection.

Author contributions

ME: Investigation, Data curation, Writing—original draft. NK: Data curation. SM: Conceptualization, Data curation. JT, MS: Investigation, Validation, Writing—review & editing, Project administration, Supervision. YI: Investigation, Conceptualization, Validation, Writing—review & editing, Project administration, Supervision. All the authors have read and approved the submitted manuscript.

Conflicts of interest

The authors declare that this study received β-cyclodextrin from Cyclo Chem Co., Ltd., which was not involved in the study design, collection, analysis, interpretation of data, the writing of this article, or the decision to submit it for publication. The authors declare that the research was conducted in the absence of commercial or financial relationships that could be construed as potential conflicts of interest.

Ethical approval

Not applicable.

Consent to participate

Not applicable.

Consent to publication

Not applicable.

Availability of data and materials

The original contributions presented in the study are included in the article, further inquiries can be directed to the corresponding author.

Funding

The author(s) declare that no financial support was received for the research, authorship, and/or publication of this article.

Publisher's note

Open Exploration maintains a neutral stance on jurisdictional claims in published institutional affiliations and maps. All opinions expressed in this article are the personal views of the author(s) and do not represent the stance of the editorial team or the publisher.

References

1. Althobaiti HM, Althobaiti H, Khan M, Alsatti H, Samarkandy SJ. The Association Between Facial Dermatosis and Face-Mask Wearing During COVID-19 in Saudi Arabia. Cureus. 2022;14:e22265. [DOI] [PubMed] [PMC]
2. Gomaa AA, Abdel-Wadood YA. The potential of glycyrrhizin and licorice extract in combating COVID-19 and associated conditions. Phytomed Plus. 2021;1:100043. [DOI] [PubMed] [PMC]
3. Santonocito D, Puglia C, Torrisi C, Giuffrida A, Greco V, Castelli F, et al. Calorimetric Evaluation of Glycyrrhetic Acid (GA)- and Stearyl Glycyrrhetinate (SG)-Loaded Solid Lipid Nanoparticle Interactions with a Model Biomembrane. Molecules. 2021;26:4903. [DOI] [PubMed] [PMC]
4. Oyama K, Kawada-Matsuo M, Oogai Y, Hayashi T, Nakamura N, Komatsuzawa H. Antibacterial Effects of Glycyrrhetinic Acid and Its Derivatives on Staphylococcus aureus. PLoS One. 2016;11:e0165831. [DOI] [PubMed] [PMC]
5. Sakata O, Fujii M, Koizumi N, Nakade M, Kameyama K, Watanabe Y. Effects of oils and emulsifiers on the skin penetration of stearyl glycyrrhetinate in oil-in-water emulsions. Biol Pharm Bull. 2014;37:486–9. [DOI] [PubMed]
6. Piquero-Casals J, Hexsel D, Mir-Bonafé JF, Rozas-Muñoz E. Topical Non-Pharmacological Treatment for Facial Seborrheic Dermatitis. Dermatol Ther (Heidelb). 2019;9:469–77. [DOI] [PubMed] [PMC]
7. Cid-Samamed A, Rakmai J, Mejuto JC, Simal-Gandara J, Astray G. Cyclodextrins inclusion complex: Preparation methods, analytical techniques and food industry applications. Food Chem. 2022;384:132467. [DOI] [PubMed]
8. Braga SS, Barbosa JS, Santos NE, El-Saleh F, Paz FAA. Cyclodextrins in Antiviral Therapeutics and Vaccines. Pharmaceutics. 2021;13:409. [DOI] [PubMed] [PMC]
9. Ho S, Thoo YY, Young DJ, Siow LF. Cyclodextrin encapsulated catechin: Effect of pH, relative humidity and various food models on antioxidant stability. LWT Food Sci Tech. 2017;85:232–39. [DOI]
10. Przybyla MA, Yilmaza G, Becer CR. Natural cyclodextrins and their derivatives for polymer synthesis. Polym Chem. 2020;11:7582–602. [DOI]

11. Cheirsilp B, Rakmai J. Inclusion complex formation of cyclodextrin with its guest and their applications. Biol Eng Med. 2016;2:1–6. [DOI]
12. Jansook P, Ogawa N, Loftsson T. Cyclodextrins: structure, physicochemical properties and pharmaceutical applications. Int J Pharm. 2018;535:272–84. [DOI] [PubMed]
13. Fenyvesi É, Vikmon M, Szente L. Cyclodextrins in food technology and human nutrition: Benefits and limitations. Crit Rev Food Sci Nutr. 2016;9;56:1981–2004. [DOI]
14. Inoue Y, Motoda A, Tanikawa T, Takao K, Arce F Jr, See GL, et al. Inclusion complexes of ursolic acid with cyclodextrin-based metal-organic framework-1 enhance its solubility. J Drug Deliv Sci Technol. 2023;89:104986. [DOI]
15. Alfei S, Schito AM, Zuccari G. Considerable Improvement of Ursolic Acid Water Solubility by Its Encapsulation in Dendrimer Nanoparticles: Design, Synthesis and Physicochemical Characterization. Nanomaterials (Basel). 2021;11:2196. [DOI] [PubMed] [PMC]
16. Inoue Y, Yoshida M, Ezawa T, Tanikawa T, Arce F Jr, See GL, et al. Inclusion Complexes of Daidzein with Cyclodextrin-Based Metal-Organic Framework-1 Enhance Its Solubility and Antioxidant Capacity. AAPS PharmSciTech. 2021;23:2. [DOI] [PubMed]
17. Prabu S, Sivakumar K, Swaminathan M, Rajamohan R. Preparation and characterization of host-guest system between inosine and β-cyclodextrin through inclusion mode. Spectrochim Acta A Mol Biomol Spectrosc. 2015;147:151–7. [DOI] [PubMed]
18. Bucur S, Niculaua M, Ciobanu CI, Lungu NC, Mangalagiu I. A Simple Synthesis Route for Selectively Methylated *β*-Cyclodextrin Using a Copper Complex Sandwich Protecting Strategy. Molecules. 2021; 26:5669. [DOI] [PubMed] [PMC]
19. Ogawa N, Higashi K, Nagase H, Endo T, Moribe K, Loftsson T, et al. Effects of cogrinding with β-cyclodextrin on the solid state fentanyl. J Pharm Sci. 2010;99:5019–29. [DOI] [PubMed]
20. Mura P, Bettinetti GP, Cirri M, Maestrelli F, Sorrenti M, Catenacci L. Solid-state characterization and dissolution properties of naproxen-arginine-hydroxypropyl-beta-cyclodextrin ternary system. Eur J Pharm Biopharm. 2005;59:99–106. [DOI] [PubMed]
21. Inoue Y, Watanabe S, Suzuki R, Murata I, Kanamoto I. Evaluation of actarit/γ-cyclodextrin complex prepared by different methods. J Incl Phenom Macrocycl Chem. 2015;81:161–8. [DOI]
22. Aigner Z, Berkesi O, Farkas G, Szabó-Révész P. DSC, X-ray and FTIR studies of a gemfibrozil/dimethyl-β-cyclodextrin inclusion complex produced by co-grinding. J Pharm Biomed Anal. 2012;57:62–7. [DOI] [PubMed]
23. Yamamoto K, Tanikawa T, Tomita J, Ishida Y, Nakata D, Terao K, et al. Characterization, Preparation, and Promotion of Plant Growth of 1,3-Diphenylurea/β-Cyclodextrin Derivatives Inclusion Complexes. ACS Omega. 2023;8:34972–81. [DOI] [PubMed] [PMC]